Data and Metadata. 2026; 5:1339
doi: 10.56294/dm20261339

ORIGINAL

Improving Autism Detection Accuracy with an Optimized Local-Asymmetric Adaptive Hybrid GCN for EEG Data

Mejora de la precisión en la detección del autismo con un GCN híbrido adaptativo asimétrico local optimizado para datos de EEG

K. Lalli[1] ✉, Senbagavalli. M[1]

[1]Department of Computer Science Engineering, Alliance School of Advanced Computing, Alliance University. Bangalore-560102, India.

Cite as: Lalli K, M S. Improving Autism Detection Accuracy with an Optimized Local-Asymmetric Adaptive Hybrid GCN for EEG Data. Data and Metadata. 2026; 5:1339. https://doi.org/10.56294/dm20261339

Submitted: 22-08-2025 **Revised:** 27-09-2025 **Accepted:** 10-12-2025 **Published:** 01-01-2026

Editor: Dr. Adrián Alejandro Vitón Castillo

Corresponding Author: K. Lalli ✉

ABSTRACT

Autism spectrum disorder (ASD) is an intricate nervous disorder typically diagnosed through the use of electroencephalography (EEG). A novel model named Dual Encoder-Balanced Conditional Wasserstein Generative Adversarial Network with Resting-state EEG-based Hybrid Graph Convolutional Network (DEBCWGAN-Rest-HGCN) was made from this context. By fixing the class imbalance and making synthetic EEG samples, it was able to detect ASD with encouraging results. However, it ignores the dynamic brain patterns recorded by task-based EEG in favor of resting-state EEG. The Rest-HGCN model also cannot successfully capture the uneven spatial and temporal aspects of EEG signals, and its fixed hyperparameters might make it less accurate in detecting different types of EEG data. This article presents a new model for finding and diagnosing ASD called the Optimized Local-Asymmetric Adaptive Hybrid GCN (OLA2HGCN). This model uses both spatial and temporal information from resting-state and task-driven EEG signals. It is based on the way autism affects brain connections and a variation amid the left and right hemispheres. The LA2HGCN can efficiently collect discrete spatiotemporal EEG information through distinct areas and hemispheres by improving the HGCN model with hierarchical feature extraction and fusion approaches. This model has a time based feature extraction approach in the cognitive prior graph branch that picks up temporal characteristics inside and between brain areas. It also has an adaptive GCN for spatial feature extraction across non-Euclidean distributions of electrodes. An attention layer shows how each hemisphere helps with ASD classification. A new Quantum Artificial Gorilla Troops Optimizer (QGTO) is also presented to help the LA2HGCN model choose the best hyperparameters. The QGTO is based on the social intelligence of gorilla tribes. It rapidly traverses intricate search spaces and achieves an equilibrium between exploration and exploitation. By adding quantum mechanics to the GTO method, it can better find its way through complicated search spaces and stay away from local optima. This makes hyperparameter selection more successful. Finally, the test results show that the DEBCWGAN- OLA2HGCN on the EEG Dataset for ASD and the ABC-CT dataset are 95,04 % and 92,27 % accurate, respectively, when compared to other algorithms.

Keywords: Autism Spectrum Disorder; Resting-State EEG; Task-Based EEG; DEBCWGAN; GCN; Quantum Mechanics; Artificial Gorilla Troops Optimizer.

RESUMEN

Este artículo presenta un nuevo modelo para la detección y el diagnóstico del TEA, denominado Red Convolucional Híbrida Adaptativa Local-Asimétrica Optimizada (OLA2HGCN). Este modelo utiliza información espacial y temporal de las señales de EEG en reposo y basadas en tareas. Se basa en la forma en que el autismo afecta las conexiones cerebrales y en la variación entre los hemisferios izquierdo y derecho. El LA2HGCN puede recopilar eficientemente información discreta de EEG espaciotemporal a través de distintas áreas y hemisferios,

mejorando el modelo HGCN con enfoques jerárquicos de extracción y fusión de características. Este modelo cuenta con un enfoque de extracción de características basado en el tiempo en la rama de grafos cognitivos previos, que capta características temporales dentro y entre áreas cerebrales. También cuenta con un GCN adaptativo para la extracción de características espaciales en distribuciones de electrodos no euclidianas. Una capa de atención muestra cómo cada hemisferio contribuye a la clasificación del TEA. También se presenta un nuevo Optimizador Cuántico Artificial de Tropas de Gorilas (QGTO) para ayudar al modelo LA2HGCN a seleccionar los mejores hiperparámetros. El QGTO se basa en la inteligencia social de las tribus de gorilas. Recorre rápidamente espacios de búsqueda complejos y logra un equilibrio entre exploración y explotación. Al incorporar la mecánica cuántica al método GTO, puede navegar mejor en espacios de búsqueda complejos y evitar los óptimos locales. Esto facilita la selección de hiperparámetros. Finalmente, los resultados de la prueba muestran que DEBCWGAN-OLA2HGCN en el conjunto de datos de EEG para TEA y el conjunto de datos ABC-CT tienen una precisión del 95,04 % y del 92,27 %, respectivamente, en comparación con otros algoritmos.

Palabras clave: Trastorno del Espectro Autista; EEG en Reposo; EEG Basado en Tareas; DEBCWGAN; GCN; Mecánica Cuántica; Optimizador de Tropas Gorilas Artificiales.

INTRODUCTION

ASD is a common neurodevelopmental disorder that usually shows up at birth or in early childhood. It is marked by problems with social contact, a lack of interests, repetitive activities, and sometimes problems with thinking.[1] For effective treatment, it is very important to get proper diagnosis. Cognitive and psychological tests are often used to diagnose ASD, however this process can take a long time and cause delays in getting a diagnosis.[2,3,4] Detecting ASD early is very important since quick therapy can help with symptoms and close the gap between children with ASD and individuals with Typical Development (TD).[5] Researchers are currently looking at the possibility of using impartial signs from Computed Tomography (CT) and Magnetic Resonance Imaging (MRI) to discover ASD early.[6]

Still, these imaging methods shouldn't be used to diagnose ASD in kids because the link between brain results and ASD traits is not well-defined. Prior research has demonstrated that when autistic child's brain grow, their EEG signals become less complex.[7,8] There are noticeable differences in the right and inner brain areas of children with autism compared to neurotypical children. These results suggest that EEG signals could give us unique and useful information about how the brains of people with autism work.[9,10] EEG signals are a more useful diagnostic method for ASD since they capture time in a complex way, are easy to use, and are cheaper than MRI and CT scans. Also, EEG is used with people of all ages and is easier to get for clinical use than MRI and CT. So, it is very important to build EEG-based algorithms for diagnosing autism so that ASD may be found and screened for early on.[11]

Researchers have used deep learning (DL) algorithms like Convolutional Neural Networks (CNNs) and Recurrent Neural Networks (RNNs) to look at EEG forms and figure out if someone has ASD in the last few decades.[12] These models have made progress in identifying ASD, but it is still crucial to use the statistical information from EEG channels correctly. CNNs can get features from multi-channel data, however they may not fully show how related the channels are in a complex way. This could make it harder for CNN/RNN built models to accurately anticipate outcomes. Consequently, the cognitive prior and the data based graph components were combined by Tang et al.[13] to create the Rest-HGCN technique aimed at ASD. Data-based graph component retains dynamic information flow traits. The cognitive prior graph component leverages EEG cerebral systems as prior graph data to acquire strong neurological connectivity forms among cerebral areas. The Rest-HGCN improves its ability to detect ASD by using attention strategies, which extract discriminatory characteristics. This strengthens the separation between healthy and ASD child.

On the other hand, the Rest-HGCN method faced challenges due to small datasets, impacting its validation. Deep learning requires large labeled datasets, but there is a lack of public EEG data for ASD detection. EEG data collection is inconsistent, leading to imbalanced samples. Data augmentation techniques like adding Gaussian noise have been used, but those may not meet the needs for synthetic EEG creation.[14] GAN-based models show promise in improving EEG signals by considering correlations between waves. Earlier GANs create EEG waves based on spectral traits, which may not capture temporal variances effectively, leading to complex data generation processes. So, a novel DEBCWGAN model with Rest-HGCN has been developed for ASD detection[15], aiming to generate minority-class EEG samples from an imbalanced dataset. This model incorporates spatiotemporal features to create synthetic examples considering electrode location correlation and time-based traits of EEG waves. The Differential Entropy (DE) traits were transformed into temporal and electrode location features, input into Variational Auto-Encoder (VAE) encoders, and decoded into synthetic

examples. Additionally, gradient penalty and L2 regularization terms were used to prevent overfitting. The Rest-HGCN was then trained to find ASD using the larger dataset.

The Rest-HGCN model only looks at resting-state EEG, while task-based EEG shows how brain patterns change during certain tasks. Also, it's hard to use Rest-HGCN to find unusual brain patterns in autism based on resting-state EEG since it is unable to capture the spatial and temporal elements of EEG data. Also, the Rest-HGCN model's predetermined hyperparameters may make it less flexible when working with different types of EEG data, which could lower its accuracy and make it harder to work with new test data, that makes it less useful in the real world.

This paper suggests a new end-to-end OLA^{2}HGCN model that can learn different spatial and temporal aspects from resting-state and task-based EEG signals. This is based on how autism affects brain connection and hemispheric asymmetry. It improves the HGCN model by employing hierarchical feature extraction and integration to understand spatial and temporal EEG information that may be separated from different brain areas and hemispheres. This model has a time-based feature extraction approach in the cognitive prior graph branch that picks up temporal characteristics inside and between brain areas. It also has an adaptive GCN for spatial feature extraction across non-Euclidean distributions of electrodes. An attention layer highlights the role of each hemisphere in classification. The QGTO is also made to find the best hyperparameters for the LA^{2}HGCN model. This optimizer uses the GTO, which is noted for being good at searching through complicated and high-dimensional spaces. The GTO algorithm is based on the social intelligence of gorilla groups. It is easy to use and can be changed, which helps it converge quickly. But it can be hard for it to get out of local optima. The GTO algorithm now includes quantum mechanics to get around this problem. This improvement makes it easier for the optimizer to find the best hyperparameters by balancing exploration and exploitation. So, the DEBCWGAN-OLA^{2}HGCN model has been shown to greatly increase the accuracy of finding and diagnosing ASD.

This part looks at recent research on using deep learning models to find people with autism by looking at their EEG data. Baygin et al.[16] built a hybrid lightweight deep feature extractor that can find ASD using EEG inputs. They used 1D Local Binary Pattern (LBP) to get information from the signals and Short Time Fourier Transform (SIFT) to make spectrogram images. The deep features from the images were extracted using pre-trained MobileNetV2, ShuffleNet, and SqueezeNet techniques. Then, feature selection was done with a dual-phased ReliefF algorithm, and the most important characteristics were categorized with a Support Vector Machine (SVM) classifier. However, the accuracy was found to be low.

Ari et al.[17] developed an automated method to distinguish ASD with the help of EEG data. At first, the Douglas-Peucker algorithm was employed for diminishing the quantity of EEG data. A sparse coding was applied to create EEG rhythm-based images. Then, an Extreme Learning Machine with Auto-Encoder (ELM-AE) was employed for augmentation. The pre-trained CNN models were used to classify ASD and healthy EEG signals, but the model may not accurately capture spatial and temporal variations, affecting detection accuracy.

Rogala et al.[18] combined traditional statistics and machine learning to classify ASD in children using EEG data. They used normal and corrected imaginary phase locking value to identify unique brain connectivity patterns in children with ASD. However, due to a small sample size, accuracy was limited. Additionally, the reliance on resting-state EEG data could miss some of the nuances in how the brain communicates with one another in ASD. Peketi et al.[19] developed a novel method that combines Variational Mode Decomposition (VMD) and SVM classifier to classify P300 EEG signals in individuals with ASD. However, a key limitation was the need to determine the number of modes for decomposition in advance, which may result in mode mixing or redundancy if not properly optimized.

Menaka et al.[20] created an improved version of the AlexNet model by incorporating Linear Frequency Cepstral Coefficients (LFCC) to identify ASD from EEG waves, with an accuracy of 90%. On the other hand, it could not learn temporal information from EEG waves, and its effectiveness depended a lot on the right hyperparameter choices. Using EEG data, Xu et al.[21] came up with a new way to find ASD. They generated Time-Series Maps of Brain Functional Connectivity (TSM-BFC) by combining temporal data from EEG signals. We used a Deep Convolutional GAN (DCGAN) to add more data. Then, a CNN-Long Short-Term Memory (LSTM) technique was utilized to find ASD by looking at the time and space aspects of EEG signals. But the accuracy was low because the sample size was limited, which made it more likely to overfit.Using EEG data, Toranjsimin et al.[22] built a model for diagnosing ASD early and without noise. They cleaned up and cut up the signals, and then they used cross wavelet transform images as input for AlexNet, GoogleNet, VGG19, ResNet50, and ResNet101. But these models had trouble capturing temporal features, which made them less accurate and less able to recall. Al-Qazzaz et al.[23] used transfer learning and hybrid CNNs to differentiate between EEG readings from those with ASD and those without. To start, the EEG signals were split into 5-second chunks and turned into 2D grayscale spectrogram images using the power spectral density method. Next, we used pre-trained CNN models including AlexNet, SqueezeNet, MobileNetV2, GoogleNet, ResNet18, ShuffleNet, and EfficientNet to get features from each spectrogram image. Decision trees, K-nearest neighbors, and SVM were used to construct hybrid models that could differentiate between normal people and people with mild, moderate, and severe ASD. Conversely,

the accuracy of these models was low due to their inability to capture temporal characteristics effectively.

The literature review reveals a gap in research on autism detection using EEG signals. Current studies focus mainly on resting-state EEG data, neglecting the insights that task-related EEG can offer. This limited focus hinders the models' ability to capture the full range of brain activity in individuals with autism. Moreover, CNN models struggle to extract and analyze the complex spatial and temporal characteristics of autism-related brain activity effectively. Also, the fixed hyperparameters in these models restrict their adaptability to the diverse nature of EEG data across patients, leading to reduced accuracy and poor generalizability. To address these issues, this study aims to develop an optimized deep learning model that can effectively capture spatial and temporal features from EEG signals. This model will also be fine-tuned to enhance its performance by optimizing hyperparameters.

METHOD

The OLA^{2}HGCN model for ASD detection and diagnosis is outlined in this section. Figure 1 illustrates a visual graphical representation for the proposed work.

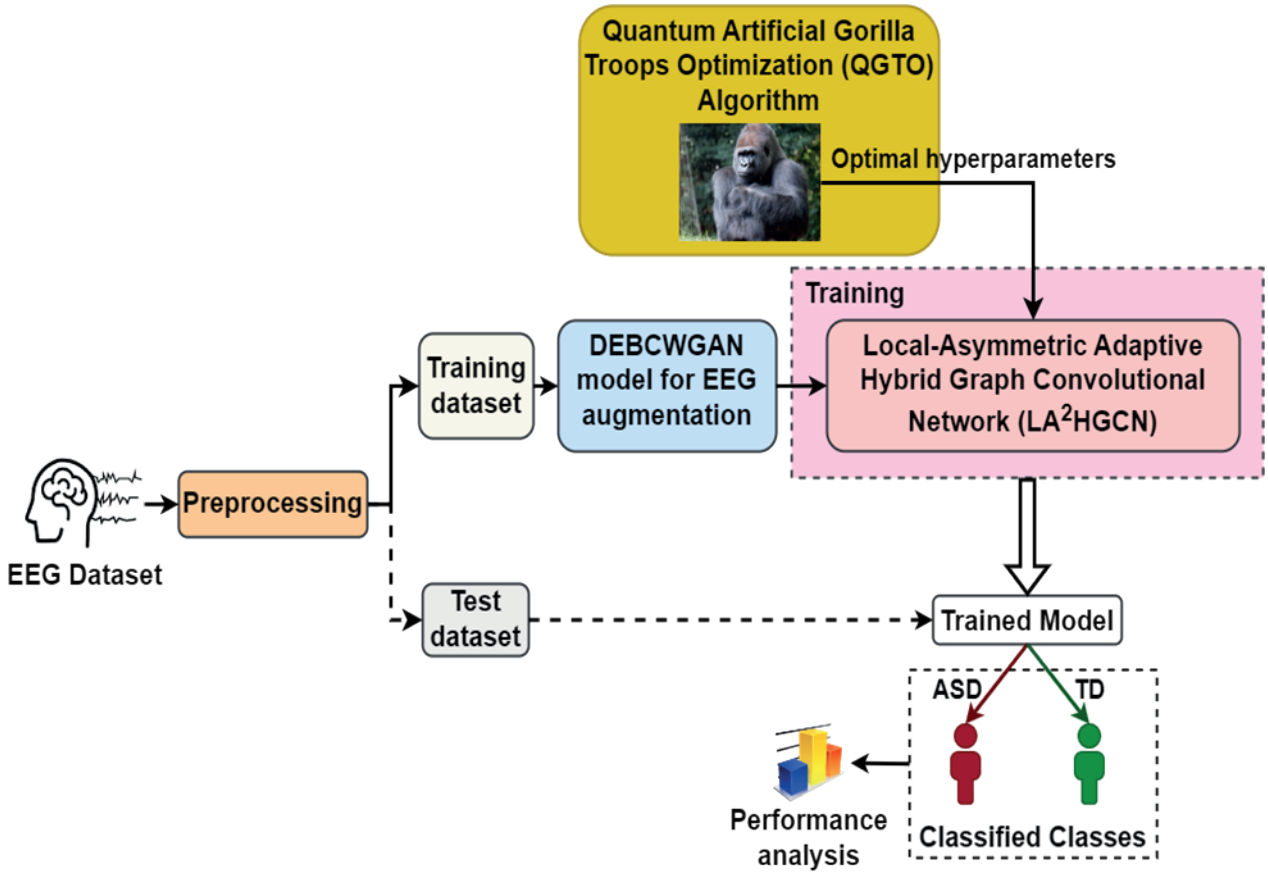

Figure 1. Schematic Representation of the suggested module

Dataset Description

This study utilizes two widely recognized datasets to gather EEG signals from children diagnosed with ASD and children who are TD:

1. EEG Dataset for ASD:[24] EEG data were collected from 28 individuals with ASD and 28 TD individuals using the Biosemi Active two EEG system. This dataset comprises recordings of eyes closed and sleeping for a 2,5-minute period. The DEBCWGAN model generates 2000 artificial EEG data (1000 from each class) using 44 training samples to improve classification performance.
2. Autism Biomarkers Consortium for Clinical Trials (ABC-CT) dataset:[25] It includes EEG and eye-tracking data from 280 ASD contributors and 119 TD contributors aged 6–11 years. EEG data was collected at three time points. The DEBCWGAN model generates 2000 artificial EEG data (1000 from each class) using 319 training samples to enhance classification performance.

Pre-processing and Augmentation

The raw EEG data are preprocessed to extract DE features from 5 frequency groups (alpha, gamma, delta,

beta, theta) for each of the 62 EEG channels. These features are segmented into 5-second windows. To capture temporal and spatial information, the data is transformed in two ways: 1) A 5-second segment with 310 dimensions (62 channels x 5 bands) for timing, and 2) A 16x16 grid representation of the 62 channels for each 5-second window to capture spatial relationships. Additionally, every electrode is connected to Cz, sampling frequency set to 1000 Hz, and electrodes' impedance is maintained below 50 kΩ. If an electrode has an impedance greater than 50 kΩ or a threshold greater than 200V while recording, an artifact detection method will be employed to identify it. These electrodes have been identified as channels with poor interpolation. The filtered signals are again equilibrated with the mean reference of two mastoids. This preprocessed data is fed to the DEBCWGAN model for data augmentation. This model uses two encoder networks to learn temporal and spatial patterns separately before combining them to generate synthetic EEG samples. Thus, it creates balanced training data to enhance the performance of the autism detection classifier.

Local-Asymmetric Adaptive Hybrid Graph Convolutional Network Model

The LA²HGCN model is designed to improve the accuracy of autism diagnosis by extracting discriminative features. Using adaptive graph convolution and the parameter-sharing mechanism of CNNs, this model is able to learn the asymmetric spatial aspects based on functional connections in the brain as well as the temporal characteristics of different brain regions. Before feeding them into a classifier, the retrieved characteristics are merged using an attention technique to optimize the differences. Figure 2 shows the general design of the LA²HGCN model that has a classifier, a global concatenation method, an asymmetric spatial feature extractor, an adaptive graph structure learner, and a regional temporal feature extractor.

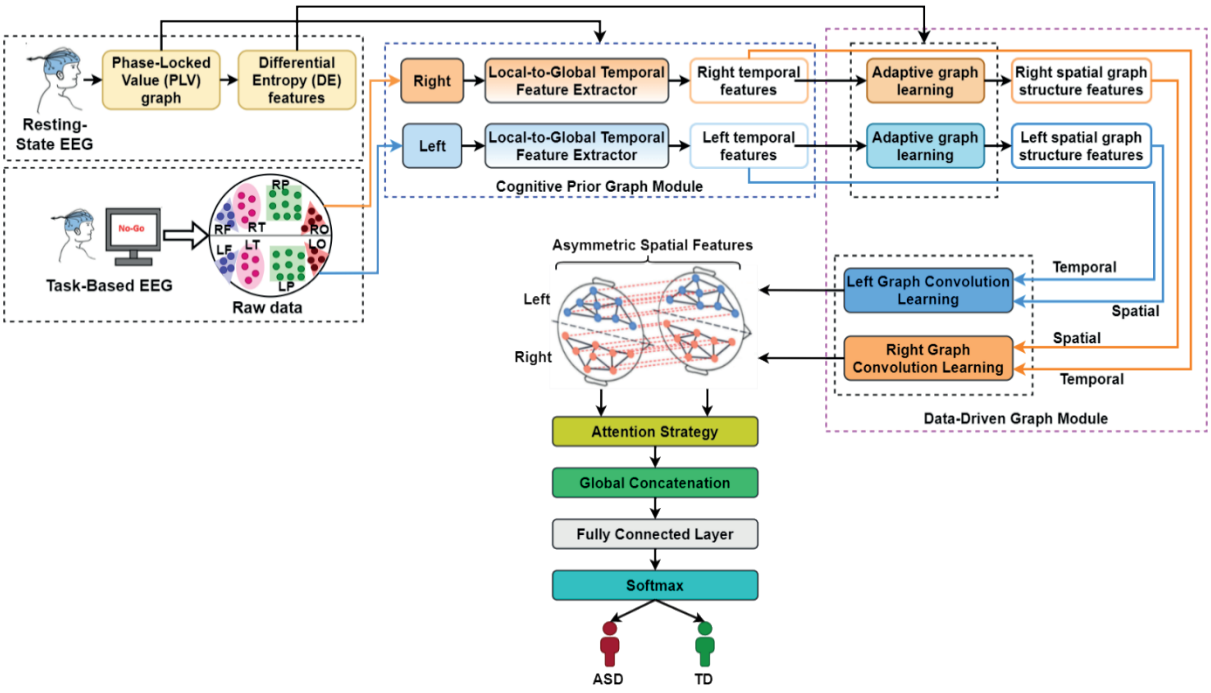

Figure 2. Architecture of LA²HGCN Model

Model Input

In this study, 46 channels are selected using the 10-10 autism criteria to encompass the four functional areas of the brain: the frontal, temporal, parietal, and occipital lobes. The left and right hemispheres of cerebral channels are symmetrically sorted to ensure comparability. Participant data is normalized to reduce differences. Data is cut to remove bad fragments and randomly selected for ten-second slices. Each participant's data is processed into 10 samples without overlap. A dimension is added to produce numerous convolution kernel (ConvKern) channels in a technique used as input to facilitate learning of features in both spatial and temporal aspects. The model input matrix is defined as:

$$X = \{X^{left}, X^{right}\} \quad (1)$$

The matrices, X^{left} and X^{right} represent EEG data from the left and right hemispheres, respectively. Each matrix has a size of c/2×point, where c is the total number of channels and point is the segment length, (i.e.,

https://doi.org/10.56294/dm20261339

1000). X^{left} and X^{right} are made up of EEG data from four brain areas in each hemisphere, which are labeled X_i^{left} and X_i^{right} for i=1,2,3,4.

Local-Temporal Feature Extractor (LTFE)

Here, 2D convolution is employed to derive time-based properties of each electrode. The convolution operation is set up using a parameter-sharing technique to make a local temporal feature extractor that is specific to the functional properties of brain areas in autism. Each electrode's time series data runs through two 2D convolution procedures. The only thing that is different between them is a collection of common variables. The LTFE model employs Convolutional (Conv) blocks in all four regions and both hemispheres to get temporal characteristics from smaller areas. The parameters of the ConvKern are shared throughout all regions of the brain. The parts of a Conv block is 2D Conv layer, an average pooling (AvgPool) layer and an activation function called ReLU. This method is described as:

$$B_i^r = \sigma\left(Avg_2\left(Conv2D(X_i^r, s_1)\right)\right) \qquad (2)$$

The variables X_i^r and B_i^r represent the raw data input and local temporal feature, respectively, for the i^th brain area of the r hemisphere in equation (2), where r is an element of the left and right hemispheres and i is an element of the 1, 2, 3 and 4 sets. The 2D convolution method Conv2D(·) uses a kernel scale of s_1=fs/2, the ReLU activation function is denoted as σ(·), and the average pooling layer Avg_2 (·) is used to lower the temporal dimension by half to prevent overfitting and increase robustness.

The EEG frequency commonly used for autism diagnosis ranges from 2Hz to 70Hz. Therefore, a ConvKern scale of (1,fs/2) is selected to capture temporal features above 2Hz. After the region's local-temporal features have been retrieved, the hemibrain's temporal features can be learned using the same convolution blocks. Prior to this, combining spatially-related brain region feature maps from the same hemisphere is essential. This method is described as:

$$B^r = [B_1^r, \ldots, B_i^r] \qquad (3)$$

The local-temporal feature extractor produces a final feature map that is computed as:

$$Tem^r = \sigma\left(Avg_2\left(Conv2D(B^r, s_2)\right)\right) \quad (4)$$

In equation (4), is a portion of the final phase of feature mapping.

Adaptive Graph Network Learning

The adjacency matrix is created by learning the neighboring feature correlations of electrodes in the technique, unlike a fixed graph structure. In this study, the graph structures of the left and right hemibrains are established separately to obtain the adjacency matrices A^{left} and A^{right}.

Let A_{ij}^{left}, A_{ij}^{right}=g(x_i,x_j) is used to depict the connections between nodes x_i and x_j, where i,j∈{1,2,…,n} represent the nodes in the hemibrain. The feature map ⟦Tem⟧^r provides vectors equivalent to nodes i and j. The function g(X_i, x_j) is computed using a learnable weight vector ω=(ω_1,ω_2,…,ω_f)∈$R^{f\times1}$ and the attributes of i and j. The ω shares variables across all node connections during the learning process. The ConvKern feature layers from previous layer averages are used to depict the graph structure of the adjacency matrix as:

$$A_{mn}^r = g(x_m, x_n) = \frac{e^{\left(\sigma\left(\omega^T|x_n - x_m|\right)\right)}}{\sum_{m=1}^{N} e^{\left(\sigma\left(\omega^T|x_m - x_n|\right)\right)}} \quad (5)$$

The ReLU activation function converts linear units into non-negative numbers. Based on a time feature map that is dynamic, the adjacency matrix is fine-tuned iteratively by total cross-entropy loss. The cross-entropy loss function is:

$$\mathcal{L}_{CE} = -\frac{1}{B}\sum_{batch=1}^{B}\sum_{class=0}^{1} y_{batch,class}\log_1 \hat{y}_{batch,class} \qquad (6)$$

Finally, A_{ij}^{left} and A_{ij}^{right} has been computed. This matrix serves as input for a graph network in graph convolutional learning.

https://doi.org/10.56294/dm20261339

Asymmetric-Spatial Feature Extractor (ASFE)

Graph convolution in EEG data involves approximating graph ConvKern (GConvKern) with the help of Chebyshev polynomials, reducing computational complexity to K, where K is the Chebyshev polynomials count used. By integrating hemibrain adjacency matrices with the time-based attributes of every node, both the left and right hemispheres' non-Euclidean spatial characteristics are acquired. The Chebyshev GConvKern with K-1 order is:

$$F_g^r = g_\theta * \mathcal{G} Tem^r = g_\theta(L) Tem^r = \sum_{k=0}^{K-1} \theta_k T_k(\tilde{L}) Tem^r \qquad (7)$$

In equation (7), g_θ symbolizes the ConvKern, *G denotes the graph convolution procedure, and $\tilde{L}$ symbolizes the normalized Laplace matrix defined as $\tilde{L}=2/\lambda_{max}$ -1, where λ_{max} denotes the maximum eigenvalue. The eigenvalue diagonal matrix of the normalized Laplace matrix, as per the criteria of the Chebyshev polynomial of the 1st class, is transformed to an interval [-1,1]. The repititive definition of the initial class of Chebyshev polynomials is as follows:

$$T_0(x) = 1, T_1(x) = x, T_{n+1}(x) = 2xT_n(x) - T_{n-1}(x) \qquad (8)$$

This is generated using a iterative formula T_k (L), which denotes the Chebyshev polynomial. Furthermore, θ_k symbolizes the Chebyshev coefficients vector.

Attention-Based Feature Concatenation

Attention strategies are employed to evaluate the spatial and temporal characteristics of the left and right brains before entering the model. Attention mechanism adjusts its attention based on influence of each hemisphere on categorization outcomes. The process is illustrated in Figure 3. Global pooling compresses global features, and the fully connected layer using activation function learns a non-linear relationship between the left and right hemispheres. EEG asymmetry features in autism are obtained through weighted averaging after fusion. These fused features are denoted as:

$$Fusion = GAP\left(Att\left(\left[F^{left}, F^{right}\right], Q\right)\right) = \frac{1}{k}\sum_{k=1}^{K}\left[\beta_1 F^{left}, \beta_2 F^{right}\right] \qquad (9)$$

In equation 9, K represents the quantity of GConvKerns, Q denotes dimension reduction ratio throughout the compression of the attention strategy and β_1,β_2 are left and right brain weights resulting after the attention strategies.

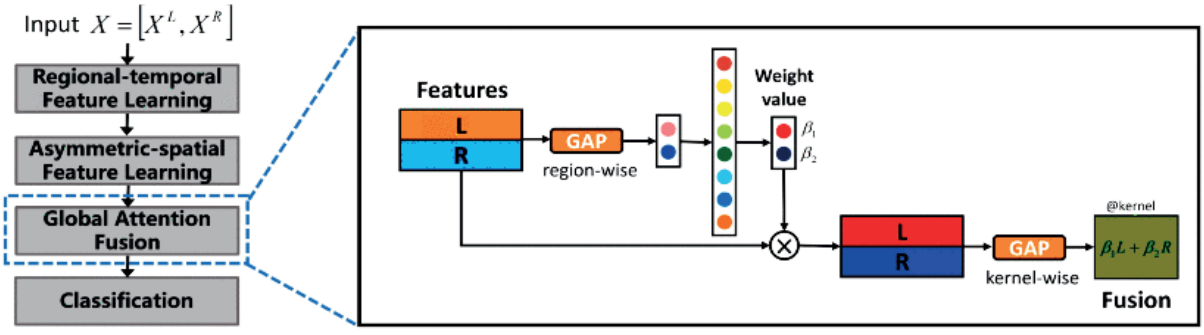

Figure 3. Attention-Based Hemibrain Feature Concatenation

Classifier

The final likelihood of an autism diagnosis is the product of training and a classification loss optimization model, like a cross-entropy loss function. A two-layer classification layer using the ReLU and Softmax functions receives the spatiotemporal fusion feature matrix as input. The output is defined as:

$$\hat{y} = Softmax(W_2 p \circ (W_1 Fusion + b_1) + b_2) \qquad (10)$$

https://doi.org/10.56294/dm20261339

Algorithm 1 LA²HGCN Technique
Input: EEG data X=[X^{left},X^{right}], True label y, and maximum iterations T:
Output: LA²HGCN recognition (yˆ)

```
Initialize: ω0←0;
for(t←1:T)
  for(r∈[L,R])
    for(i=1:4)
      Obtain ith area output Bir using equation (2);
      Obtain Bi using equation. (3) and time based hybrid learning result Tem^r using Eq.(4);
    end for
    Obtain A_mn^r using equation. (5);
    Obtain graph Conv learning result F_g^r using equation (7);
  end for
  Obtain the concatenated weighted sum using attention strategy as equation (9);
end for
Obtain yˆ by equation. (10);
End
```

Thus, the LA²HGCN model is trained to distinguish between children with ASD and TD. The model's hyperparameters are optimized by QGTO to improve detection accuracy, as detailed in the next section.

Quantum Artificial Gorilla Troops Optimization (AGTO) for Hyperparameter Selection

The AGTO model is inspired by the social behavior of gorillas. Gorillas typically congregate in groups headed by an adult male called silverback, due to the white hair on their back. The group typically includes adult females and their offspring. The male gorilla is responsible for defending territory, making decisions, and guiding the group in finding food. Rivalry for territory and resources is common among gorillas, with male-female interactions being close and female-female interactions more distant.[26]

Exploration Phase

In the gorilla community, a silverback gorilla leads decision-making. Gorillas explore various locations for food, including familiar and unfamiliar situations. The silverback gorilla represents the ideal solution during the exploration phase. Additionally, three strategies are activated during this stage, as described in equation (11). The variable ρ, ranging [0,1], determines the migration plan for unidentified locations. If rand<ρ, the current gorilla's location moves to an anonymous place, allowing for better coverage of the problem space and a complete distribution of solutions. If rand≥ρ, two other mechanisms are activated. If rand≥1/2, the gorilla moves towards other gorillas, enhancing exploration. If rand<1/2, the gorillas migrate to known positions, aiding in escaping local optima.

$$GX(t+1) = \begin{cases} (u_b - l_b) \times r_1 + l_b, & rand < \rho \\ (r_2 - C) \times X_r(t) + L \times H, & rand \geq \frac{1}{2} \\ X(t) - L \times \Big(L \times \big(X(t) - GX_r(t)\big)\Big) + r_3 \times \big(X(t) - GX_r(t)\big), & rand < \frac{1}{2} \end{cases} \quad (11)$$

In equation (11), GX(t+1) represents the gorilla candidate location vector for the succeeding t iteration, X(t) denotes the present gorilla location vector, r_1,r_2,r_3 and rand are random values in [0,1] altered in every iteration, u_b and l_b denote variables' upper and lower limits, X_r is a unsystematically nominated gorilla in the population, and GX_r is a unsystematically nominated vector of gorilla candidate locations that includes locations updated in all stages. Moreover, C,L, and H are determined as follows:

$$C = \cos(2 \times r_4) + 1 \times \left(1 - \frac{T}{T_{max}}\right) \quad (12)$$

In equation (12), T is the present iteration, T_{max} is the maximum iteration, and r_4 denotes uniform distribution in 0 to 1. While value of C changes somewhat in the later stages, it changes considerably in the beginning. This allows for greater randomness in the early stage to explore a global optimal solution, while in the later stage, it decreases to facilitate rapid convergence.

$$L = C \times l \quad (13)$$

https://doi.org/10.56294/dm20261339

In equation (13), l represents a random integer produced by a normal distribution between -1 and 1, while L is a parameter that models the leadership of a silverback gorilla. Silverback gorillas may make errors in foraging or group management due to their inexperience. By following a leader, they can gain valuable experience and achieve greater stability. Equation (13) is a way to simulate the influence of a silverback gorilla's leadership. Also, H is determined as follows:

$$H = Z \times X(t) \quad (14)$$

$$Z = [-C, C] \quad (15)$$

Upon completion of this phase, the fitness values (i.e., detection accuracy) of GX and X are determined. When the fitness value of GX(t) is smaller than that of X(t), the location of GX(t) will swap the location of X(t).

Exploitation Phase

The GTO algorithm calls upon two behaviors throughout its exploitation phase: accompanying the silverback and competing with mature female gorillas. The silverback gorilla leads the group, makes choices, directs movements, and ensures safety. The silverback's decisions are followed by all of the group's gorillas. However, as the silverback may weaken or die, a new leader may emerge through rivalry within the group. The choice between these behaviors is determined by the value in equation 12. If C≥W, following the silverback is selected; otherwise, rivaling with adult female gorillas is chosen, where the optimization procedure begins with the setting of a parameter, W.

Following the Silverback

The recently formed gorilla group is led by a young and strong silverback, with other young males following his lead effectively. They obey his commands to search for food in different areas and stick together as a cohesive unit. This strategy is implemented when C≥W is met, using equation 16 for simulation.

$$GX(t+1) = L \times M \times (X(t) - X_{silverback}) + X(t) \quad (16)$$

$$M = \left(\left| \frac{1}{N} \sum_{i=1}^{N} GX_i(t) \right|^{g} \right)^{1/g} \quad (17)$$

$$g = 2^{L} \quad (18)$$

In equations (16,17,18), In iteration t, GX_i (t) is the candidate position vector of all gorillas, and $X_{silverback}$ is the location vector of the silverback gorilla (best answer).

2. Rivaling with Adult Female Gorillas

If C<W, the exploitation phase will use the second behavior. During the adolescent years, gorilla males engage in mating wars with other gorillas in order to increase their population and choose adult females. Disputes inside the group might escalate into physical altercations and drag on for days. This behavior is simulated by equation (19), as follows:

$$GX(t) = X_{silverback} - (X_{silverback} \times Q - X(t) \times Q) \times A \quad (19)$$

$$Q = 2 \times r_5 - 1 \quad (20)$$

$$A = \beta \times E \quad (21)$$

In equations. (19,20,21,22), Q represents the intensity of the simulated gorilla's rivalry, r_5,rand are the random numbers in [0,1] for a normal distribution, E mimics the effect of aggression on the solution dimension, ß is the parameter established before to the optimization process, and A is the coefficient vector that mimics the intensity of rivalry. Any value from a normal distribution in the problem dimension can equal E if rand is greater than or equal to 1/2. On the other hand, E might represent a normal distribution random number.

Upon completion of this phase, a group formation operation is carried out to estimate the fitness value of all GX solutions. If the fitness value of GX(t) is less than X(t), then GX(t) solution is utilized as the X(t) solution.

https://doi.org/10.56294/dm20261339

The silverback is selected as the best option that was found from the whole population.

Quantum Mechanism

This study integrates quantum mechanics into the GTO algorithm to improve its capability to balance exploration and exploitation in the search space. Quantum mechanics is used as an additional strategy for location updating, particularly during the exploitation stage, to enhance the algorithm's performance in discovering optimal solutions. The Monte Carlo technique is employed to determine the new solution x_{new} such as updating location of each gorilla as follows:

$$z = \frac{r_1(w)\times GX(t)+r_2(1-w)\times GX(t)}{r_1+r_2} \quad (23)$$

$$GX(t+1) = \begin{cases} z + \alpha \times \left(Mbest_i - X(t)\right) \times \ln\left(\frac{1}{u}\right), & h \geq \frac{1}{2} \\ z - \alpha \times \left(Mbest_i - X(t)\right) \times \ln\left(\frac{1}{u}\right) & Or\ else \end{cases} \quad (24)$$

$$\alpha = \frac{0.5\times(T_{max}-T)}{T-0.5} \quad (25)$$

In equations (23) & (25), α represents the contraction-expansion coefficient, which is gradually decreased through the curse of iterations to control the convergence rate and find the global optimum, u and w follow a normal distribution with parameters between 0 and 1, while h takes on a value between 0 and 1 at random. The mean of the X_silverback locations is also known as Mbest, which stands for the population's best result. It is determined as:

$$Mbest = \frac{1}{N}\sum_{i=1}^{N} GX_i(t) \quad (26)$$

A flowchart of this QGTO is presented in figure 4. Thus, the QGTO selects the optimal hyperparameters of the LA²HGCN model to improve model training and ASD detection accuracy. Table 1 displays the optimal hyperparameters selected by the QGTO algorithm for the LA²HGCN model.

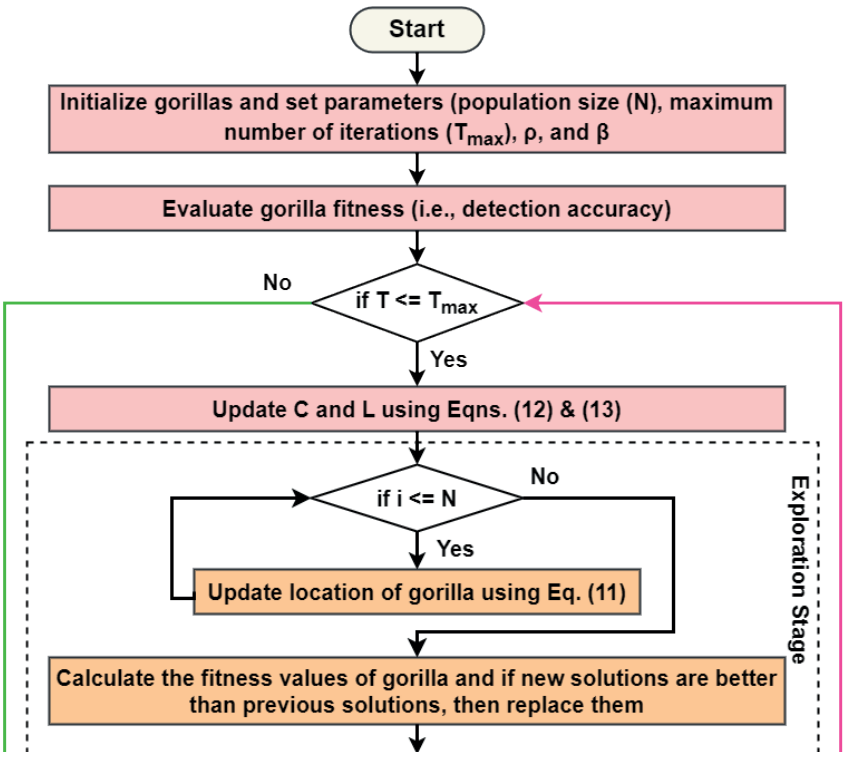

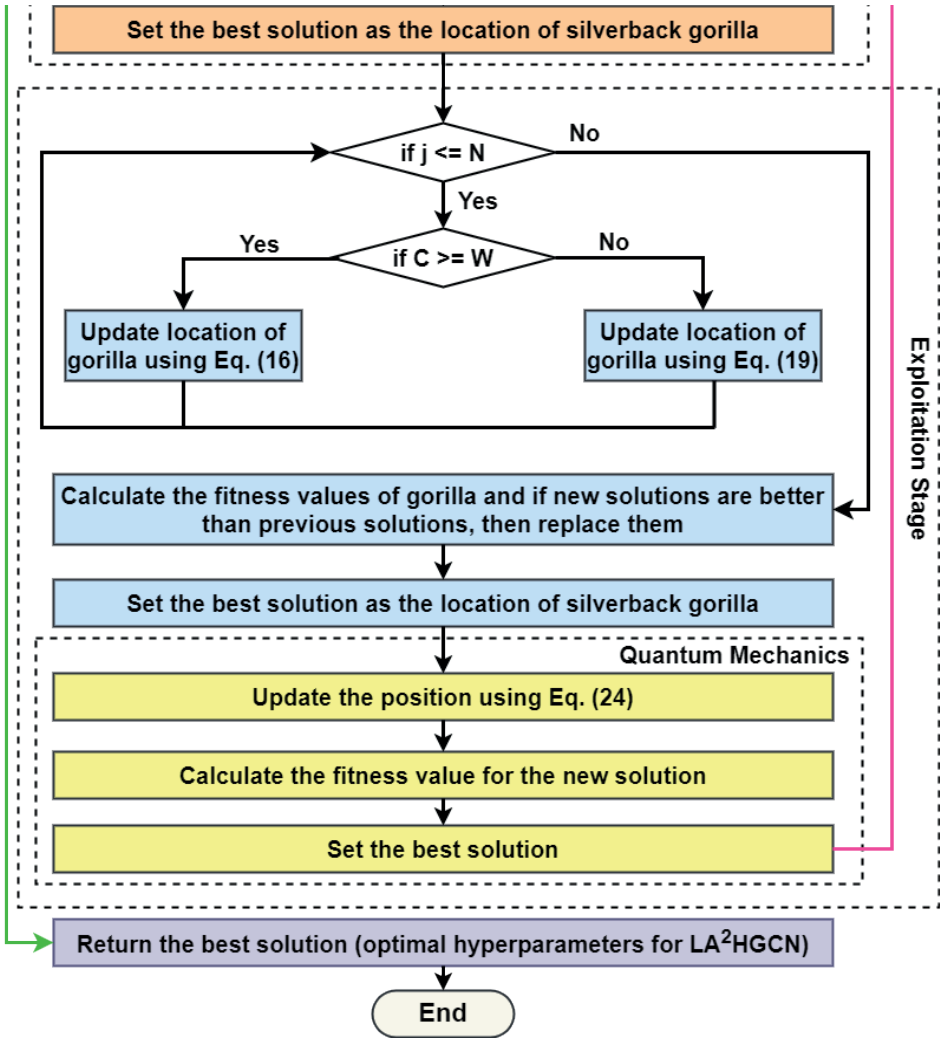

Figure 4. Flowchart of QGTO Algorithm for Optimal Hyperparameter Selection

Table 1. List of Hyperparameters for LA²HGCN Model for ASD Detection and Diagnosis

Parameters	Search Space	Optimal Range
No. of graph convolutional layers	[2,3,4]	3
Number of hidden layers	[1, 2]	1
Training rate	[0.0001, 0.1]	0,01
Dropout rate	[0,2, 0,3, 0,4, 0,5]	0,5
Number of epochs	[100, 300]	200
Batch size	[32, 64, 128, 256, 512]	256
Optimizer	[Stochastic gradient descent, Adam]	Adam
Loss	[Cross-entropy, mean squared error]	Cross-entropy

RESULTS

This division assesses the robustness of suggested DEBCWGAN-OLA²HGCN technique using two distinct EEG datasets as described in Section 3.1. The model's performance is compared with existing models, such as Rest-HGCN,[14] DEBCWGAN-rest-HGCN,[15] VMD-SVM,[19] Improved AlexNet,[20] and DCGAN-CNN-LSTM.[21] The experiment is carried out on a laptop with an Intel® Core TM i5-4210 CPU @ 3GHz, 4GB RAM, and a 1TB HDD on Windows 10 64-bit. The two datasets were used to implement all existing and proposed models in MATLAB 2019b in order to quantify performance enhancements.

Performance Evaluation Measures

The effectiveness of ASD detection models can be assessed by means of the subsequent measures:

- Accuracy is the proportion of exactly recognized cases among the total cases assessed.

https://doi.org/10.56294/dm20261339

$$Accuracy = \frac{True\ Positive\ (TP) + True\ Negative\ (TN)}{TP + TN + False\ Positive\ (FP) + False\ Negative\ (FN)} \quad (27)$$

In equation (27), TP occurs when the network correctly identifies a subject with ASD as having ASD. TN occurs when the network correctly identifies a subject without ASD as not having ASD. FP arises when the network mistakenly identifies a subject without ASD as having ASD. FN arises when the network mistakenly identifies a subject with ASD as not having ASD.

- Precision, recall, and F1 score are determined as follows:

$$Precision = \frac{TP}{TP + FP} \quad (28)$$

$$Recall = \frac{TP}{TP + FN} \quad (29)$$

$$F1 = \frac{2 \times Precision \times Recall}{Precision + Recall} \quad (30)$$

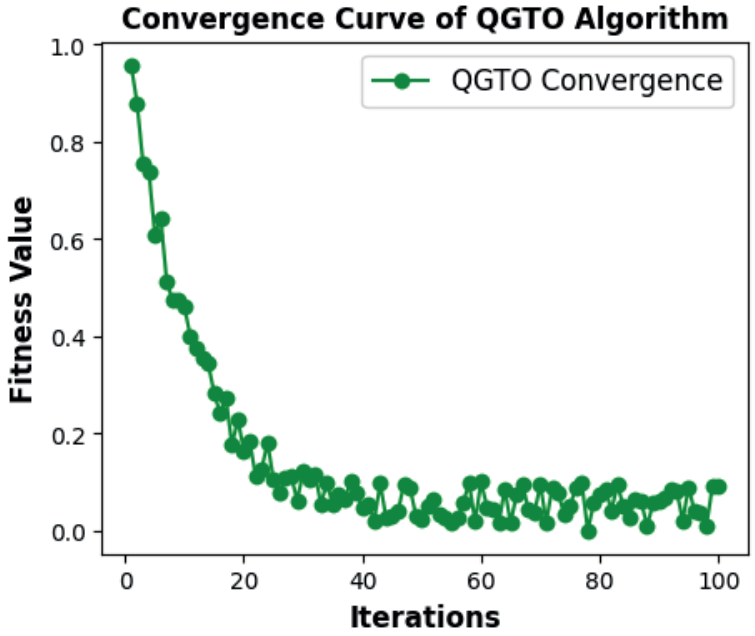

Figure 5. Convergence Curve of QGTO Algorithm

Figure 5 displays the convergence curve of the QGTO model, showcasing the improvement in fitness value over iterations. The curve demonstrates a rapid initial enhancement followed by a gradual plateau as the algorithm converges towards an optimal solution. This indicates the QGTO's effective balance between exploration and exploitation, facilitating effective exploration of the search domain while evading neighborhood optimums.

Figure 6 compares the DEBCWGAN-OLA²HGCN model with existing models on the EEG Dataset for ASD. The DEBCWGAN-OLA²HGCN outperforms other models in detecting children with ASD due to effective training using a large-scale dataset. Compared to VMD-SVM, improved AlexNet, DCGAN-CNN-LSTM, Rest-HGCN, and DEBCWGAN-Rest-HGCN, the proposed model shows an increase in precision by 42,25 %, 32,77 %, 23,84 %, 13,81 %, and 10,65 %, recall by 42,51 %, 26,28 %, 21,56 %, 14,02 %, and 0,84 %, F1-score by 42,39 %, 29,44 %, 22,7 %, 13,92 %, and 2,84 %, and accuracy by 42,55 %, 26,72 %, 23,56 %, 14,05 %, and 3,68 %, respectively.

Figure 7 compares the proposed DEBCWGAN-OLA²HGCN model with existing models on the ABC-CT dataset for classifying children with ASD. The DEBCWGAN-OLA²HGCN model outperforms other models due to effective training with a large-scale dataset. Compared to VMD-SVM, improved AlexNet, DCGAN-CNN-LSTM, Rest-HGCN, and DEBCWGAN-Rest-HGCN, the anticipated technique attains a higher precision, recall, F1-score, and accuracy. Precision is improved by 13,72 %, 8,73 %, 6,56 %, 4,32 %, and 0,52 %, recall by 17,73 %, 10,67 %, 6,5 %, 4,4 %, and 0,6 %, F1-score by 15,73 %, 9,71 %, 6,53 %, 4,37 %, and 0,57 %, and accuracy by 29,18 %, 19,24 %, 13,13 %, 10,73 %, and 4,73 %, respectively.

https://doi.org/10.56294/dm20261339

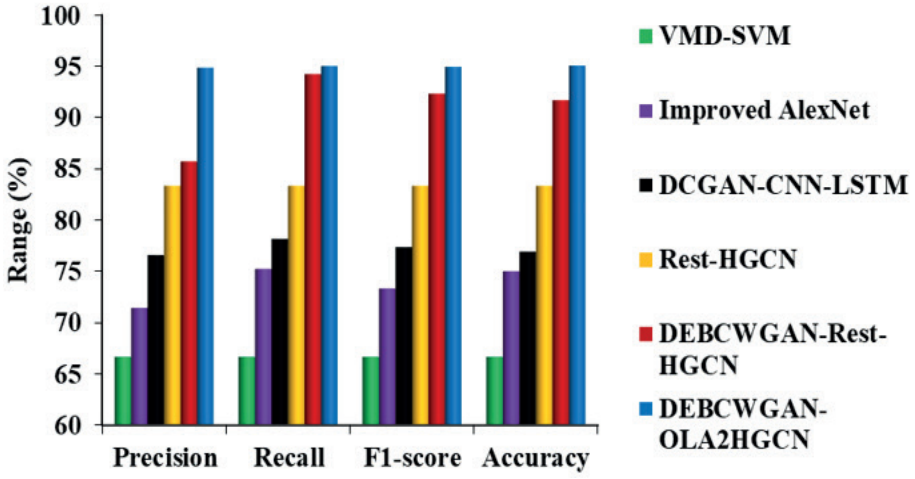

Figure 6. Comparison of DEBCWGAN-OLA²HGCN Model against Existing Models on EEG Dataset for ASD

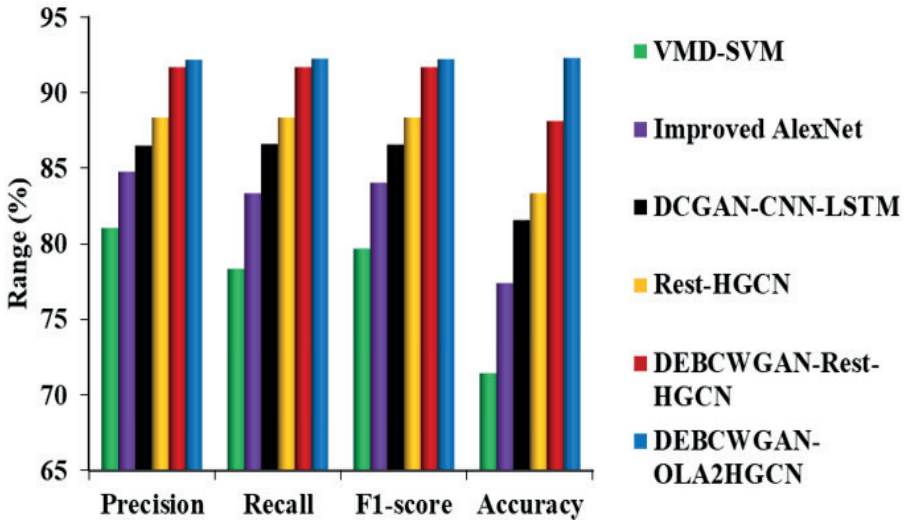

Figure 7. Comparison of DEBCWGAN-OLA²HGCN Model against Existing Models on ABC-CT Dataset

CONCLUSIONS

The study shows how the OLA²HGCN model and DEBCWGAN can work together to improve the detection of ASD by using both resting-state and task-based EEG data. The LA²HGCN model made it easier to acquire different spatial and temporal aspects from EEG recordings. The addition of a new QGTO to the LA²HGCN improved its hyperparameters, which led to better accuracy in classifying ASD than earlier methods. These new results point to a viable path for future research and therapeutic use. The DEBCWGAN-OLA²HGCN model was able to correctly identify 95,04 % of EEG data for ASD and 92,27 % of ABC-CT data for ASD, showing that it might be used to locate ASD early and accurately.

BIBLIOGRAPHIC REFERENCES

1. Dharia A, Mandal A, Kondekar AS, Naik N, Gaikwad BA. A brief about autism spectrum disorders for nurses and other peripheral health workers. IP Int J Med Paediatr Oncol. 2021;7(2):90–97.

2. Kaufman NK. Rethinking “gold standards” and “best practices” in the assessment of autism. Appl Neuropsychol Child. 2022;11(3):529–540.

3. Abrahamson V, Zhang W, Wilson PM, Farr W, Reddy V, Parr J, et al. Realist evaluation of Autism ServiCe Delivery (RE-ASCeD): which diagnostic pathways work best, for whom and in what context? Findings from a rapid realist review. BMJ Open. 2021;11(12):e051241.

4. Kaiser AP, Chow JC, Cunningham JE. A case for early language and behavior screening: implications for policy and child development. Policy Insights Behav Brain Sci. 2022;9(1):120–128.

5. Smythe T, Zuurmond M, Tann CJ, Gladstone M, Kuper H. Early intervention for children with developmental disabilities in low- and middle-income countries: the case for action. Int Health. 2021;13(3):222–231.

6. Lima AA, Mridha MF, Das SC, Kabir MM, Islam MR, Watanobe Y. A comprehensive survey on the detection, classification, and challenges of neurological disorders. Biology (Basel). 2022;11(3):469.

7. Milovanovic M, Grujicic R. Electroencephalography in assessment of autism spectrum disorders: a review. Front Psychiatry. 2021;12:686021.

8. Tan G, Xu K, Liu J, Liu H. A trend on autism spectrum disorder research: eye tracking–EEG correlative analytics. IEEE Trans Cogn Dev Syst. 2022;14(3):1232–1244.

9. Salehi F, Jaloli M, Coben R, Nasrabadi AM. Estimating brain effective connectivity from EEG signals of patients with autism disorder and healthy individuals by reducing volume conduction effect. Cogn Neurodyn. 2022;16(3):519–529.

10. Kang J, Xie H, Mao W, Wu J, Li X, Geng X. EEG connectivity diversity differences between children with autism and typically developing children: a comparative study. Bioengineering (Basel). 2023;10(9):1030.

11. Zhang Y, Zhang S, Chen B, Jiang L, Li Y, Dong L, et al. Predicting the symptom severity in autism spectrum disorder based on EEG metrics. IEEE Trans Neural Syst Rehabil Eng. 2022;30:1898–1907.

12. Jui SJJ, Deo RC, Barua PD, Devi A, Soar J, Acharya UR. Application of entropy for automated detection of neurological disorders with electroencephalogram signals: a review of the last decade (2012–2022). IEEE Access. 2023;11:71905–71924.

13. Tang T, Li C, Zhang S, Chen Z, Yang L, Mu Y, et al. A hybrid graph network model for ASD diagnosis based on resting-state EEG signals. Brain Res Bull. 2024;206:110826.

14. Rommel C, Paillard J, Moreau T, Gramfort A. Data augmentation for learning predictive models on EEG: a systematic comparison. J Neural Eng. 2022;19(6):066020.

15. Lalli K, Senbagavalli M. Enhancing deep learning for autism spectrum disorder detection with dual-encoder GAN-based augmentation of electroencephalogram data. Salud Cienc Tecnol Ser Conf. 2024;3:958.

16. Baygin M, Dogan S, Tuncer T, Barua PD, Faust O, Arunkumar N, et al. Automated ASD detection using hybrid deep lightweight features extracted from EEG signals. Comput Biol Med. 2021;134:104548.

17. Ari B, Sobahi N, Alçin ÖF, Sengur A, Acharya UR. Accurate detection of autism using Douglas–Peucker algorithm, sparse coding-based feature mapping and convolutional neural network techniques with EEG signals. Comput Biol Med. 2022;143:105311.

18. Rogala J, Żygierewicz J, Malinowska U, Cygan H, Stawicka E, Kobus A, Vanrumste B. Enhancing autism spectrum disorder classification in children through the integration of traditional statistics and classical machine learning techniques in EEG analysis. Sci Rep. 2023;13(1):21748.

19. Peketi S, Dhok SB. Machine learning enabled P300 classifier for autism spectrum disorder using adaptive signal decomposition. Brain Sci. 2023;13(2):315.

20. Menaka R, Karthik R, Saranya S, Niranjan M, Kabilan S. An improved AlexNet model and cepstral coefficient-based classification of autism using EEG. Clin EEG Neurosci. 2024;55(1):43–51.

21. Xu Y, Yu Z, Li Y, Liu Y, Li Y, Wang Y. Autism spectrum disorder diagnosis with EEG signals using time series maps of brain functional connectivity and a combined CNN–LSTM model. Comput Methods Programs Biomed. 2024;250:108196.

22. Toranjsimin A, Zahedirad S, Moattar MH. Robust low complexity framework for early diagnosis of autism spectrum disorder based on cross wavelet transform and deep transfer learning. SN Comput Sci. 2024;5(2):231.

23. Al-Qazzaz NK, Aldoori AA, Buniya A, Ali SHBM, Ahmad SA. Transfer learning and hybrid deep convolutional neural networks models for autism spectrum disorder classification from EEG signals. IEEE Access. 2024;12:64510-64530.

24. Dickinson A, Jeste S, Milne E. Electrophysiological signatures of brain aging in autism spectrum disorder. Cortex. 2022;148:139–151.

25. McPartland JC, Bernier RA, Jeste SS, Dawson G, Nelson CA, Chawarska K, et al.; Autism Biomarkers Consortium for Clinical Trials. The autism biomarkers consortium for clinical trials (ABC-CT): scientific context, study design, and progress toward biomarker qualification. Front Integr Neurosci. 2020;14:16.

26. Abdollahzadeh B, Soleimanian Gharehchopogh F, Mirjalili S. Artificial gorilla troops optimizer: a new nature-inspired metaheuristic algorithm for global optimization problems. Int J Intell Syst. 2021;36(10):5887-5958.

FINANCING

None.

CONFLICT OF INTEREST

None.

AUTHORSHIP CONTRIBUTION

Conceptualization: K. Lalli, Senbagavalli. M.
Data curation: K. Lalli, Senbagavalli. M.
Formal analysis: K. Lalli, Senbagavalli. M.
Drafting - original draft: K. Lalli, Senbagavalli. M.
Writing - proofreading and editing: K. Lalli, Senbagavalli. M.